IEEE Access
Multidisciplinary | Rapid Review | Open Access Journal

Received August 19, 2021, accepted August 29, 2021, date of publication September 3, 2021,
date of current version September 15, 2021.

Digital Object Identifier 10.1109/ACCESS.2021.3109879

Multi-UAV Path Planning Based on Fusion of Sparrow Search Algorithm and Improved Bioinspired Neural Network

QINGLI LIU, YANG ZHANG, MENGQIAN LI, ZHENYA ZHANG, NA CAO, AND JIALE SHANG

Communication and Network Laboratory, Dalian University, Dalian 116622, China

Corresponding author: Qingli Liu (lql0808@sina.com)

ABSTRACT Aiming at the problems of low stability of path planning, inability to avoid dynamic obstacles, and long path planning for multi unmanned aerial vehicles (UAV) in mountainous environment, a path planning method for UAV was proposed based on the fusion of Sparrow Search Algorithm (SSA) and Bioinspired Neural Network (BINN). The method first scans the flight environment and smoothes the surface, then raises it to obtain the safe surface, and uses SSA to find a series of nodes with the lowest comprehensive cost on the safe surface. Then, B-spline curves are used to fit these nodes, so that the planned path is smooth to meet the flight requirements of the UAV. When the dynamic obstacle is detected in the predetermined trajectory, the improved BINN method is used to carry out local path replanning to achieve the purpose of dynamic obstacle avoidance. Computer simulation results demonstrate that the fusion algorithm can plan a collision-free path in a mountainous environment, and the planned path is smooth and short. Compared with the Artificial Bee Colony Algorithm (ABC) and Dragonfly Algorithm (DA), the fusion algorithm has obvious advantages in the stability of path planning and planned path length, and has the ability of dynamic obstacle avoidance.

INDEX TERMS Path planning, multi-UAV, sparrow search algorithm, bioinspired neural network, safe surface.

I. INTRODUCTION

In recent years, UAVs have been widely used in various military and civilian missions due to their small size, lightweight, fast speed, and low cost of equipment [1]–[4]. Therefore, the important technologies of UAVs attract the attention of researchers, such as task allocation [5], communication network [6], path planning [7], and formation technology [8]. Path planning is the key and foundation of success in UAV missions. This paper mainly studies the real-time path planning of multi-UAV in mountainous environments. This problem is somewhat challenging because a long-distance complex environment needs to ensure the planned path is feasible, has low computational complexity, and avoids dynamic obstacles.

The path planning of UAVs mainly consists of two parts: environment modeling and path planning method. Conventional environmental modeling methods include Grid Maps [9], Voronoi graphs [10], and Artificial Potential Field [11]. The Grid Map is easy to model the environment, but for long flight paths, search space is too large, and it is difficult to define the size of the grid. Especially in 3-D space, the modeling will be more complex and there will be more grids [12], [13]. L proposed a method to reduce the height size and transform the 3-D mesh into a 2-D mesh, but it is still only applicable to a small environment [14]. Compared with the Grid Map, the Voronoi reduces search space, but the accuracy is also reduced. At the same time, the environment changes and it is difficult to update the model [15]. Therefore, the Voronoi is not suitable for an environment with dynamic obstacles. Artificial Potential Field can be used in dynamic environments [16], but in a complex environment, there is a problem of not finding the path [17]. Du establishes a dynamic environment model by designing a variable threshold to dynamically define the repulsion force of the obstacle, but the modeling is still too complex in the face of a complex environment [18]. In the long-distance mountainous environment, the staff map through the satellite first, and the planner can scan the region with the satellite to obtain the corresponding digital map. Fan

The associate editor coordinating the review of this manuscript and approving it for publication was Cong Pu.

used the two-dimensional cubic convolution interpolation method to preprocess the digital map [19]. Hu proposed a comprehensive smoothing algorithm [20], through which the comprehensive equivalent surface could be obtained, and then the height could be raised to generate a safe surface. The algorithm was used to plan the path on the surface, and the collision-free track could be obtained. This method is more suitable for long-distance path planning and easier to be applied in a real scene.

At present, the research methods of path planning can be divided into two categories: Global path planning and local path planning. Global path planning refers to obtaining a feasible path in a given environment through intelligent optimization algorithms or Mathematical Programming [21], In general, path planning is made for the given environment first, and then the planned route is implanted into the UAV system for off-line flight, which has low computational requirements for the UAV and relatively simple engineering application. With the rapid development of intelligent optimization algorithms, many intelligent optimization algorithms are used in path planning. Such as the Cuckoo Search algorithm(CS) [22], the Bat algorithm [23], the Grey Wolf Optimization algorithm(GWO) [24], the Genetic algorithm [25], and the Quantum Particle Swarm Optimization algorithm(QPSO) [26]. In [27], the Simulated Annealing algorithm is introduced to improve the A* algorithm for global path planning, which reduces planning time and search scope of the A* algorithm and solves the problem of long path planning time for UAV. However, it is difficult to ensure an optimal path in a complex environment. Wang used the global optimization ability of the Artificial Bee Colony (ABC) algorithm to solve the problem that the traditional A* algorithm was difficult to obtain the optimal path [28], but the ABC algorithm had the disadvantage of the locally optimal solution and low stability. Li decomposes and connects the obstacle map to form multiple convex polygons based on the convex decomposition principle of concave polygons, and then uses the ABC algorithm to search for the optimal path in all the connected domains to avoid the local optimum [29]. However, none of the above methods can solve the problem of avoiding dynamic obstacles.

Local path planning is to select the next feasible direction of the UAV according to the current environment and constraints. Because the calculation force of UAV is low, the calculation amount of this method should not be too complicated. Zhang introduced path memory to improve the Artificial Potential Field, which avoided the traditional Artificial Potential Field method easily falling into local minimum value [16]. Ulises *et al.* proposed to use the membrane pseudo-bacterial potential field (MemPBPF) algorithm to evolve the parameters required by the artificial potential field method, which achieved good results in obstacle avoidance and path smoothing [30]. Most of the above methods are suitable for small environments. However, it was difficult to ensure that the planned path was globally optimal and time-consuming, and it was not suitable for UAVs to make long-distance path planning in a mountainous environments. Chang introduced Q-learning to improve the dynamic window algorithm and increased the success rate of the dynamic window algorithm for path planning in the unknown mountainous environment [31]. However, the calculation of the algorithm is more complex, and it does not apply to the low computational power of the UAV, and the path of local path planning does not have the global optimal.

To overcome the global path planning cannot avoid the dynamic obstacles and local planning to the UAV calculation force requirements and the planned path does not meet the requirements of mountainous environment flight. In this paper, a path planning method combining global programming and local programming is proposed. This method combines the Sparrow Search algorithm(SSA) [32] and the Biologically Inspired Neural Network algorithm(BINN) [33]. In the proposed method, the safe surface map was used to construct global motion space [20], and the key nodes were searched on the safe surface using SSA. Then the B-spline Curves were used to smooth the planned path [34]. When a dynamic obstacle was detected, BINN was activated to replan the path to complete the local obstacle avoidance function. The path obtained through SSA can ensure global optimization. When dynamic obstacles are detected while flying in a predetermined path, local path reprogramming is carried out. After avoiding the dynamic obstacles, continue to fly in a predetermined path, to reduce the computational force requirement of the UAV.

The main contributions of the paper are as follows: (1) A method fused SSA and improved BINN is proposed to solve the problem that it is difficult for multi-UAV to obtain a safe, short path and avoid dynamic obstacles in a mountainous environment. The two methods promote each other and greatly improve the performance and extend function. (2) SSA was used for global path planning, and high activity values of corresponding neurons were set to avoid BINN falling into local optimum by using a global predetermined trajectory. (3) The structure of BINN's neurons was improved and a buffer layer was added to make obstacle avoidance better. (4) The fusion method reduces the computing power requirement of airborne computers and is suitable for practical applications.

This paper is divided into the following sections: Section II introduces the Flight space modeling and comprehensive cost model. In Section III, A multi-UAV path planning method based on fused SSA and improved BINN is proposed. In the IV section, the simulation analysis is carried out, and the comparison with the ABC algorithm and DA verifies the feasibility and high performance of the proposed method. Finally, Section V is comprised of the conclusion.

II. FLIGHT SPACE MODELING AND COMPREHENSIVE COST MODEL

To reach the target safely, the UAV needs to achieve collision-free flight under the conditions of total flight length constraints, threat zone distance constraints, mountainous

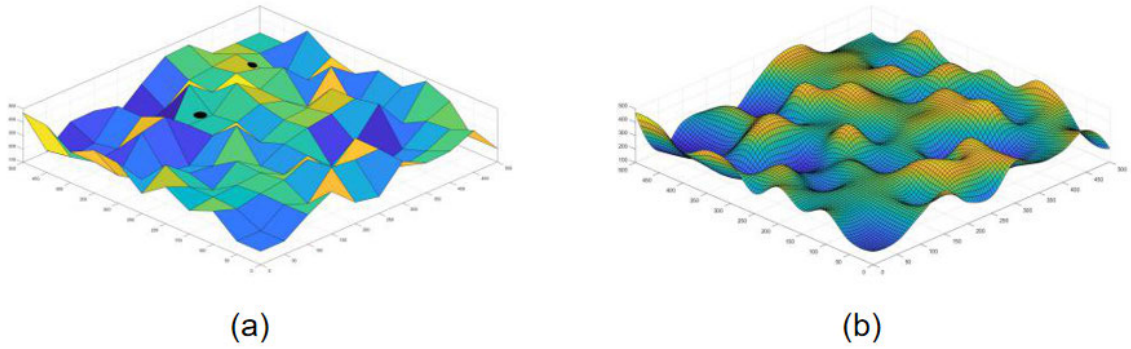

FIGURE 1. Global modeling diagram. (a) Original mountainous map, (b) Safe surface diagram.

environment constraints, and adjacent UAV distance constraints. This chapter mainly describes the UAV flight space modeling and comprehensive cost model.

A. FLIGHT SPACE MODELING

The flight space modeling studied in this paper is divided into two parts: global space modeling and local space modeling.

1) GLOBAL SPACE MODELING

In the global space, the mountainous environment of path planning is shown in Fig. 1 (a). Because the real terrain environment is complex, with deep valleys and steep mountains, the direct path planning in this environment requires higher flight requirements of the UAV, which is prone to collision. In this paper, a comprehensive smoothing algorithm proposed in [20] was adopted to limit and smooth the slope of the terrain and the curvature of the valley, to reduce the flight difficulty of the UAV. After smoothing, a smooth surface $C(x, y)$ was obtained, as shown in Fig.1 (b). Based on the smooth surface, the height h is raised to generate a safe surface $S(x, y)$. h is the minimum height of the UAV from the ground.

$$S(x, y) = C(x, y) + h \tag{1}$$

The safe surface is higher than the mountain. When flying, the UAV needs to keep a certain distance from the mountain to achieve a safe flight. When the flying height of the UAV is lower than the safe surface, it will collide with the mountain, and the path planning on the safe surface can reduce the probability of the UAV hitting the mountain and increase the flight safety of the UAV.

2) LOCAL SPACE MODELING

When the UAV flies to a certain location, the sensor detects the dynamic obstacle, then the local path replanning is started, and local modeling needs to be carried out according to the current environment. In local space, a 3 * 3 * 3 mesh map composed of neurons is established, and the connection vein of each neuron is shown in Fig.2. There are 17 alternative navigable directions of the UAV, which are represented by neuron Na. When the UAV is in the current position, it will

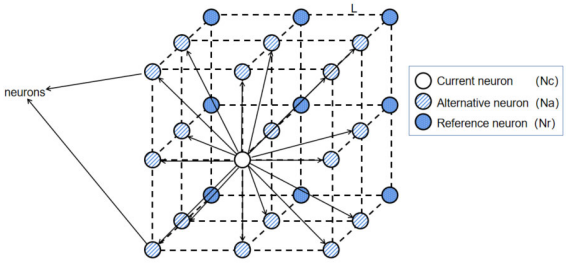

FIGURE 2. Local modeling diagram.

not only check the information of alternative neuron Na but also the information of reference neuron Nr. When the neuron Nr behind Na is occupied by obstacles, the neuron activity information of Na will be reduced. The additional reference neuron Nr can be used as a buffer for the dynamic obstacle avoidance of the UAV and improve the success rate of the obstacle avoidance of the UAV.

When the UAV starts local obstacle avoidance, the forward information is probed through the sensor and then expressed as the state information of each neuron. The state information of alternative neuron A_s is defined as Formula (2), and the state information of reference neuron R_s is defined as Formula (3).

$$A_s = \begin{cases} 2\,E & \text{target location} \\ E & \text{movable position} \\ -2\,E & \text{obstacle position} \\ 0 & \text{UAV position} \end{cases} \tag{2}$$

$$R_s = \begin{cases} -2E & \text{obstacle position} \\ 2\,E & \text{target location} \\ 0 & \text{otherwise} \end{cases} \tag{3}$$

B. COMPREHENSIVE COST MODEL

Within the threat zone, there are threats such as enemy radar detection, As shown in Fig.3, the threat zone is a cylinder formed by a threat source $O\,(x_o, y_o, z_o)$ and its action radius R_1. The UAV can only go around this range, but cannot go over it. Therefore, in the path from the key node x to the key node x + 1, the Euclides distance between any point

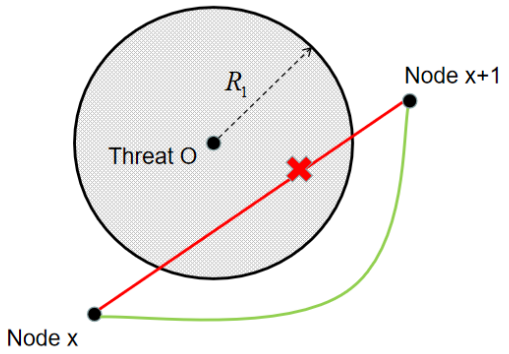

FIGURE 3. Constraint diagram of threat zone distance.

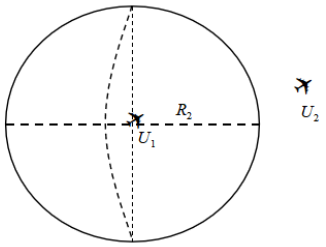

FIGURE 4. Constraint diagram of adjacent UAV distance.

$T\ (x_t, y_t, z_t)$ and threat source O shall meet the following requirements:

$$R_1 < \sqrt{(x_t - x_o)^2 + (y_t - y_o)^2 + (z_t - z_o)^2} \tag{4}$$

As shown in Fig.4, multi-UAVs need to maintain a safe distance while flying. Although different flight starting points and different timing sequences are set at the beginning of the aircraft, global path planning could cause two UAVs to collide. Therefore, it is necessary to set the minimum distance to the UAV. A sphere is built with the UAV as the center and the minimum distance R_2 as the radius. The Euclides distance of two adjacent $U_1\ (x_1, y_1, z_1)$ and $U_2\ (x_2, y_2, z_2)$ should meet the following requirements:

$$R_2 < \sqrt{(x_1 - x_2)^2 + (y_1 - y_2)^2 + (z_1 - z_2)^2} \tag{5}$$

To simulate UAV flight in the real environment as much as possible, relevant constraints are set according to the effect of total flight length l_{max} and minimum turning radius r_{min} on the actual flight of UAV. Therefore, the sum of the flying path l_i of each key node should meet the following requirements:

$$l_{max} > \sum_{i=0}^{\text{node}} l_i \tag{6}$$

In the planned path, the minimum radius of curvature is C, then the minimum turning radius r_{min} should meet the following requirements:

$$r_{min} \leq C \tag{7}$$

In this paper, the SSA algorithm is used to solve the path planning problem in global space, and the constraints include threat zone distance constraint, adjacent UAV distance constraint, total flight length constraint, and minimum turning radius constraint. The above four constraints constitute the total constraint function F_{cost}:

$$F_{cost} = \coprod_{i=1}^{4} f_i \cdot \omega_i \tag{8}$$

where f_i is the constraint expression of Equations (4), (5), (6) and (7), ω_i is the weight of each constraint, and the optimal weight is obtained through multiple simulation adjustments. The key point of an optimal solution is the minimum value of the constraint function.

III. PROPOSED SOLUTIONS

In this paper, the method of integrating SSA and improving BINN is used for multi-UAV path planning, The whole path planning problem is divided into two parts: global programming and local programming. In global programming, SSA is used to search a series of key nodes with the lowest comprehensive cost on the safe surface, and then B-spline curves were used to fit the key nodes to obtain the predetermined trajectory. When the UAV is flying, a sensor will be used to detect the environmental information ahead all the time, and local path planning will be started when a dynamic obstacle is detected ahead. Local path planning takes the current position as the starting node, the predetermined trajectory is used as the target area direction and uses the improved BINN as the local planning method. The overall planning flow chart is shown in Fig.5.

A. CALCULATE GLOBAL KEY NODES BASED ON SSA

To improve the efficiency of solving global critical track points, the SSA is used to solve the key nodes with the lowest comprehensive cost in the safe surface. SSA algorithm is a new kind of swarm intelligence optimization algorithm, which is designed according to the foraging characteristics of the sparrow population. Compared with algorithms such as Bat algorithm, GWO algorithm, Whale Optimization algorithm, Dragonfly Algorithm (DA) and Locust Optimization algorithm [35], SSA Algorithm has excellent stability and convergence in single-mode and multi-mode test functions. Because the position update of the SSA algorithm is jumping and discontinuous, it effectively avoids falling into the local optimum. The specific optimization steps are as follows:

In the SSA, the more fitness producer sparrow gets the food first. Since the producer sparrow is responsible for finding food for the entire sparrow population and providing food directions for all the join sparrows. As a result, the producer sparrow has a larger food search area than the entrant sparrow. The position update formula for each generation of Producer is as follows:

$$x_{i,d}^{t+1} = \begin{cases} x_{i,d}^{t} \cdot \exp\left(\dfrac{-i}{\alpha \cdot iter_{max}}\right), & R_2 < ST \\ x_{i,d}^{t} + Q \cdot L, & R_2 \geq ST \end{cases} \tag{9}$$

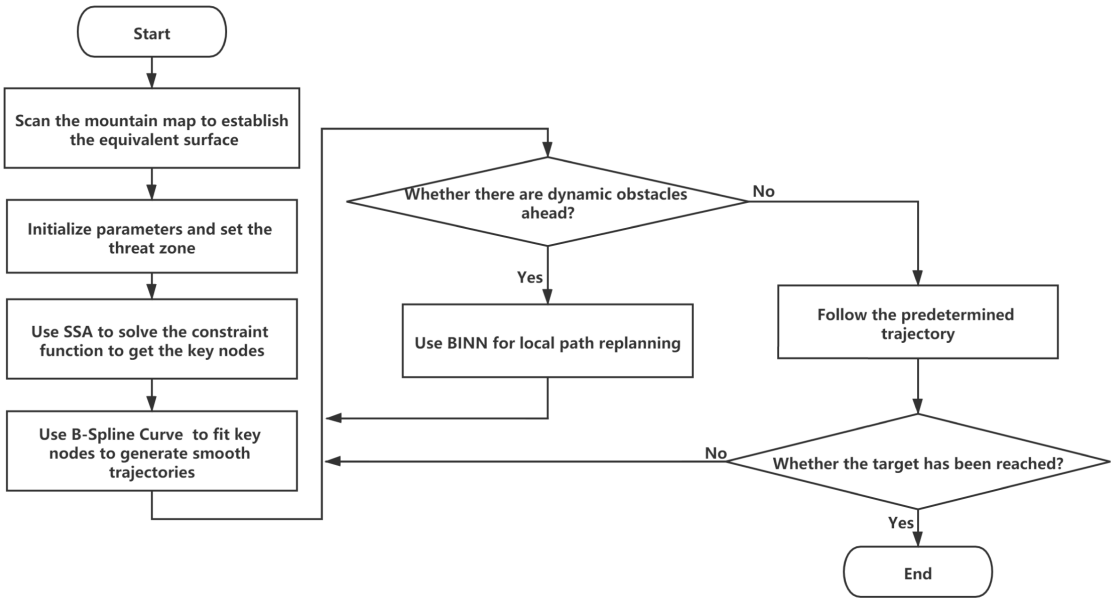

FIGURE 5. Work flow diagram.

where $x_{i,d}^t$ denotes the d-dimensional position of the ith individual in the t generation of the population, $\alpha \in (0, 1]$ is a uniform random number, $R_2 \in [0, 1]$ denotes warning value, $ST \in [0.5, 1.0]$ denotes the alert threshold, Q is a standard normally distributed random number, L denotes a matrix of 1 * d, $iter_{max}$ denotes the maximum number of iterations.

For scroungers sparrows, in the process of searching for food, some of the participating sparrows will observe the producer sparrows all the time. If the producer sparrow finds food, the scrounger's sparrow will fly around. The Scroungers position update formula is as follows:

$$x_{i,j}^{t+1} = \begin{cases} Q \cdot \exp\left(\dfrac{x_w^t - x_{i,j}^t}{i^2}\right), & i > \dfrac{n}{2} \\ x_p^{t+1} + \left|x_{i,j}^t - x_p^{t+1}\right| \cdot A^+ \cdot L, & otherwise \end{cases} \tag{10}$$

where x_w^t denotes the worst position of sparrows in the current population, and x_p^{t+1} denotes the optimal position of sparrows in the current population. A denotes a matrix of 1 * d in which each entry is randomly assigned either 1 or -1, and $A^+ = A^T\left(AA^T\right)^{-1}$.

When the entire sparrow population is threatened by a natural predator, it triggers an anti-predation mechanism: shrinking toward a central safe position. The anti-predation behavior formula is as follows:

$$x_{i,j}^{t+1} = \begin{cases} x_b^t + \beta \cdot \left|x_{i,j}^t - x_b^t\right|, & f_i > f_b \\ x_{i,j}^t + K \cdot \left(\dfrac{\left|x_{i,j}^t - x_w^t\right|}{(f_i - f_w) + \varepsilon}\right), & f_i = f_b \end{cases} \tag{11}$$

where β is the step size control parameter, obeying the normal distribution random number with a mean of 0 and variance of 1. $K \in [-1, 1]$ is a uniform random number, f_i denotes the fitness value of the current sparrow individual. f_b and f_w are the current global best and worst fitness values, respectively, ε is an extremely small constant to avoid the denominator being 0.

B. LOCAL PATH REPLANNING BASED ON BINN

The local path planning method adopts improved BINN, which is derived from the circuit model and action potential transfer formula of nerve cell membrane proposed by Hodgkin and Huxley [36]. Grossberg built on that and applied it to areas such as motion control and path planning [37]. At present, many scholars have applied this method to the path planning of UAVs. Compared with artificial potential field and dynamic window algorithm, BINN has low computational cost and high obstacle avoidance success rate, which is very suitable for path planning in an unknown environment. But in some cases, there will be wrong path judgment, planning path twists and turns [38]. NI uses the dragonfly algorithm to optimize the activity of BINN's neurons, to avoid the UAV falling into the local optimum [39]. However, the computation is heavy and the global optimum of the planned path cannot be guaranteed. In this paper, the activity of target neurons is strengthened by the predetermined trajectory of global planning and the network model is adjusted to improve the method, which can avoid the BINN algorithm falling into the local optimal, the planned path is smoother and the algorithm is more efficient.

When the sensor detects the presence of dynamic obstacles in front of the UAV during its flight, local path replanning will be initiated. The replanning takes the current position as the starting point and the direction of the predetermined

trajectory as the target area. When the sensor detects that there is no dynamic obstacle ahead and the UAV returns to the predetermined trajectory, local path planning ends.

In local planning, a 3-D mesh model is first constructed. In this model, as shown in Fig.2, a grid cell represents a neuron, and the information of each neuron is updated in real-time in the unit of seconds. Each second maps the activity information of the neuron according to environmental information detected by the sensor, and each neuron connects with adjacent neurons to form an active-transmitting network.

In the traditional BINN model, the UAV was placed in the center of 26 neurons, and it spent one-third of the time calculating information of the neurons that were moving back. Moreover, it could only perceive environmental information of one step at a time, and the success rate of avoiding dynamic obstacles was low. In a flight with a predetermined trajectory, the UAV does not travel backward, so placing the UAV in the center of the first section in BINN modeling can detect the two-step environment, making the information from each neuron more valuable.

$$\frac{dx_i}{dt} = -Ax_i + (B - x_i)\, S_i^e - (D - x_i)\, S_i^i \tag{12}$$

where x_i denotes the activity value of the ith neuron, A controls the decay rate of the neuron, B and D denotes the upper and lower limits of the neuron activity. S_i^e denotes excitatory excitation, S_i^i denotes inhibitory excitation, and its formula can be expressed as follows:

$$S_i^e = [A_S]^+ + \sum_{j=1}^{n} \omega_{ij} \left[x_j\right]^+ + [R_S]^+ \tag{13}$$

$$S_i^i = \left([A_S]^- + [R_S]^-\right) \tag{14}$$

A_s and R_s are external incentives obtained according to the environment, and their values are assigned from formula (2) and formula (3). ω_{ij} is the connection weight of the ith neuron and the jth neuron. In this paper, the Angle between two neurons is taken as the standard. The smaller the angle, the greater the weight. $[A_s]^+$ represent excitatory excitation, take the positive value, $[A_s]^-$, $[R_s]^-$ represent inhibitory excitation, take the negative value. $n = 17$ denotes 17 alternative neurons.

The activity value of each Alternative Neuron can be calculated by the above formula. The path selection strategy of UAV is as follows:

$$P_n \Leftarrow x_n = \max \ \ (x_i, i = 1, 2, \ldots, k) \tag{15}$$

In the above formula, k denotes the number of neurons adjacent to the neuron where the UAV is currently located, which is 17 in this paper. x_n denotes the most active neuron at present, and the P_n denotes the location of the neuron. When the UAV selects a path, it compares the activity of neighboring neurons and selects the most active neuron as the next step location. Repeat the above steps until the local path planning is completed when no dynamic obstacles are detected ahead and the predetermined trajectory of the global planning is returned. Because the calculation of BINN is simple, and the reference path direction will enhance the activity of the corresponding neurons, it avoids the disadvantage of falling into local optimization when conventional algorithm planning.

C. PATH SMOOTHING STRATEGY BASED ON B-SPLINE CURVE

After the SSA algorithm is used to get the key nodes, a B-spline curve fitting is used to connect the key nodes to make the planned flight path smooth and meet the flight constraints of the UAV. B-spline curves are parametric functions, and their construction is based on mixing functions. Its parameter construction provides the ability to produce non-monotonic curves. Its function expression is as follows:

$$C(u) = \sum_{i=0}^{n} P_i \cdot N_{i,p}(u) \tag{16}$$

In the above formula, P_i denotes the control vertex, $N_{i,p}(u)$ is the i-th p-order B-spline basis function corresponding to the P_i. $p \geq 1$, $U = \{u_0, u_1, \ldots, u_p, u_{p+1}, \ldots, u_n, u_{n+p}\}$, which is a nondecreasing sequence composed of $n + p + 1$ numbers in the interval [0, 1], u_i is called a node, set U is called a node vector, the beginning and end values are generally 0 or 1. If $u_i = u_{i+1} = \cdots = u_{i+p-1}$, then u_i is a multiple node of degree p, $N_{i,p}(u)$ is usually computed by a recursive formula for Cox-deBoor:

$$N_{i,0} = \begin{cases} 1 & u_i \leq u \leq u_{i+1} \\ 0 & \text{otherwise} \end{cases} \tag{17}$$

$$N_{i,p}(u) = \frac{u - u_i}{u_{i+p} - u_i} N_{i,p-1}(u) + \frac{u_{i+p+1} - u}{u_{i+p+1} - u_{i+1}} N_{i+1,p-1}(u) \tag{18}$$

If the denominator of either of the fractions is zero, that fraction is defined to have zero value. From the above formula, we can calculate the value of each basis function.

B-spline curves can be divided into uniform B-spline curves, quasi-uniform B-spline curves, piecewise Bezier curves and non-uniform B-spline curves. In this paper, the quasi-uniform B-spline curve is adopted: the node values at both ends are 0 and 1, and the repetition is based on the order p by adding 1, and all the inner nodes are evenly distributed, for example, $u_0 = \cdots = u_p = 1, 0.1, 0.2, \ldots 0.8, 0.9, u_{n+1} = \cdots = u_{n+p+1} = 1$. Its fitting effect is shown in Fig.6:

In summary, the pseudo-code of the fusion algorithm in this paper is shown in the Algorithm (see Fig.7).

IV. SIMUATION EXPERIMENTS AND DISCUSSION

To verify the feasibility and effectiveness of the method of integrating SSA and improving BINN, the simulation experiment was carried out on the Matlab platform, on a computer with the i7-7700HQ CPU and 16G memory. The main research content of this paper is the path planning of multi-UAV, which does not involve UAV formation control.

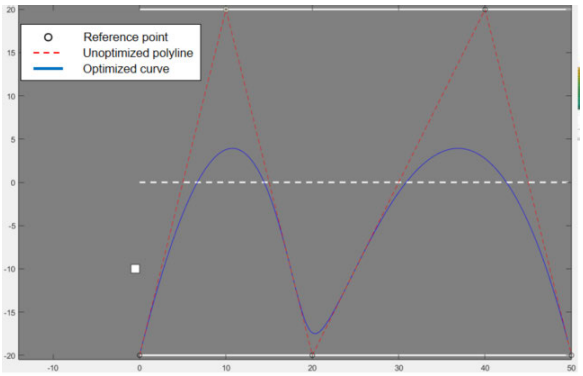

FIGURE 6. Quasi-uniform B-spline curve with 5 control points of order 3.

Algorithm : Multi-UAV Path Planning Based on SSA and Improved BINN

```
Initialization
for t= 1:Iteration
    Sort the fitness values to find the current best and worst fitness values
    R2=rand(1)        % Randomly generate the warning value R2
  for i= 1:PD         % Pd is the number of producers
    Update the Producer sparrow position by (9)
  end for
  for i= (PD+1):n
    Updates the Scroungers sparrow position by (10)
  end for
  for i= 1:SD         % SD is the number of sparrows that perceive danger
    Updates the sparrow position by (11)
  end for
end for
  B spline curves are used to connect the key nodes
for i = 1:node
  if(obstacle_flag=1):      % If the radar detects an obstacle
    Initialize the neuron activity value
    target=i+1; % Sets the next global node to be the target point of the local
programming
    while Reach the target point do
      Use (2) and (3) to assign value to the state information of each neuron
according to the environmental information
      Calculates the activity value of each alternative neuron by (12)
      Selects the neighboring neuron with the highest activity as the next step
length by (15)
      Update the location of neurons
    end while
  end if
end for
```

FIGURE 7. The pseudo code of the proposed fusion algorithm.

Therefore, the formation control of multi-UAV is simplified. To avoid collisions between UAVs, each UAV takes off at different coordinate points, and takeoff time has the sequence. The simulated environment map is a simulation of the real mountainous environment. The parameters of the proposed method and the simulation parameters in this study are listed in Table 1.

A. STATIC ENVIRONMENT EXPERIMENT

To test the performance of the proposed fusion algorithm, a static experiment is carried out first. The starting coordinates of five UAVs are (20, 20, 200), (40, 40,200), (0, 0, 200), (40, 0, 200) and (0, 40, 200) respectively. The target coordinate is (500, 500, 300), the coordinates of the two threat zones are (210, 185), (390, 410), and the threat radius is

TABLE 1. Parameters of the proposed method.

Parameters	Values	Remarks
N_distance	28	The distance between each node
Min_H	40	Minimum flight altitude
L_max	1000	Maximum path length
UAV_r	5	Safe distance of UAV
UAV_v	30m/s	UAV flight speed
Weight	[1 0.01 0.3]	The constraint weight of path length, ground height and included Angle
NP	100	Sparrow population size
P_percent	0.2	Producer sparrow of the weight
R2	0.8	Sparrow warning value
Iteration	20	Number of algorithm iterations
A	0.2	Decay rate of neuronal activity value
B	100	Upper limit of neuronal activity
D	100	Lower limit of neuronal activity
E	100	A scalar of neuronal activity values

TABLE 2. Set the mission information and environment information for the test.

Test environment	Target Q_t(x,y,z)	Obstacles O(x,y,z,r_1)
Env1	(500,500,300)	(210,185,399,20),(390,410,356,20)
Env2	(500,500,300)	(140,160,330,20),(137,290,160,20), (400,410,370,20),(460,360,240,5)
Env3	(500,500,300)	(140,160,330,20),(137,290,160,20), (400,410,370,20),(460,360,240,20)
Env4	(240,500,280)	(130,90,345,20),(130,250,235,20)
Env5	(500,320,320)	(100,100,350,20),(210,180,370,20), (430,150,270,20)
Env6	(500,0,320)	(100,100,350,20),(210,180,370,20), (430,150,270,20)

20 meters. The results are shown in Fig.8. In Fig.8(a) and Fig.8(b), we can see the flight trajectory of UAV in the mountain. Fig.8(c) shows the bottom view of the mountain, and the absence of the trajectory line of the UAV in the figure means that the UAV did not cross the mountain. Fig.8(d) shows that the flight trajectory of the five UAVs is relatively uniform and smooth, avoiding key mountains and threat zone and successfully arriving at the target area. It can be proven that the trajectory planned by this method is smooth and does not cross the mountain.

B. STATIC ENVIRONMENT CONTRAST EXPERIMENT

To test the advantages of the proposed fusion algorithm, comparative experiments were carried out. In Table 2, the mission information and environment information for path planning are shown, The mission information is represented by the starting coordinate and the ending coordinate Q_t, the starting coordinates of five UAVs are (20, 20, 200), (40, 40, 200), (0, 0, 200), (40, 0, 200) and (0, 40, 200) respectively in each experiment. The environmental information is composed of different mountainous maps and threat zone O, the information O is given by the Threat source position and its corresponding radius r_1 in (x, y, z, r_1) format. Each environment configuration is a map instance designed to evaluate the performance and accuracy of the proposed fusion algorithm; these instances were labeled as Env1, Env2, . . . , Env6.

To make a comparison between the proposed fusion algorithm and the ABC and DA algorithms, we considered

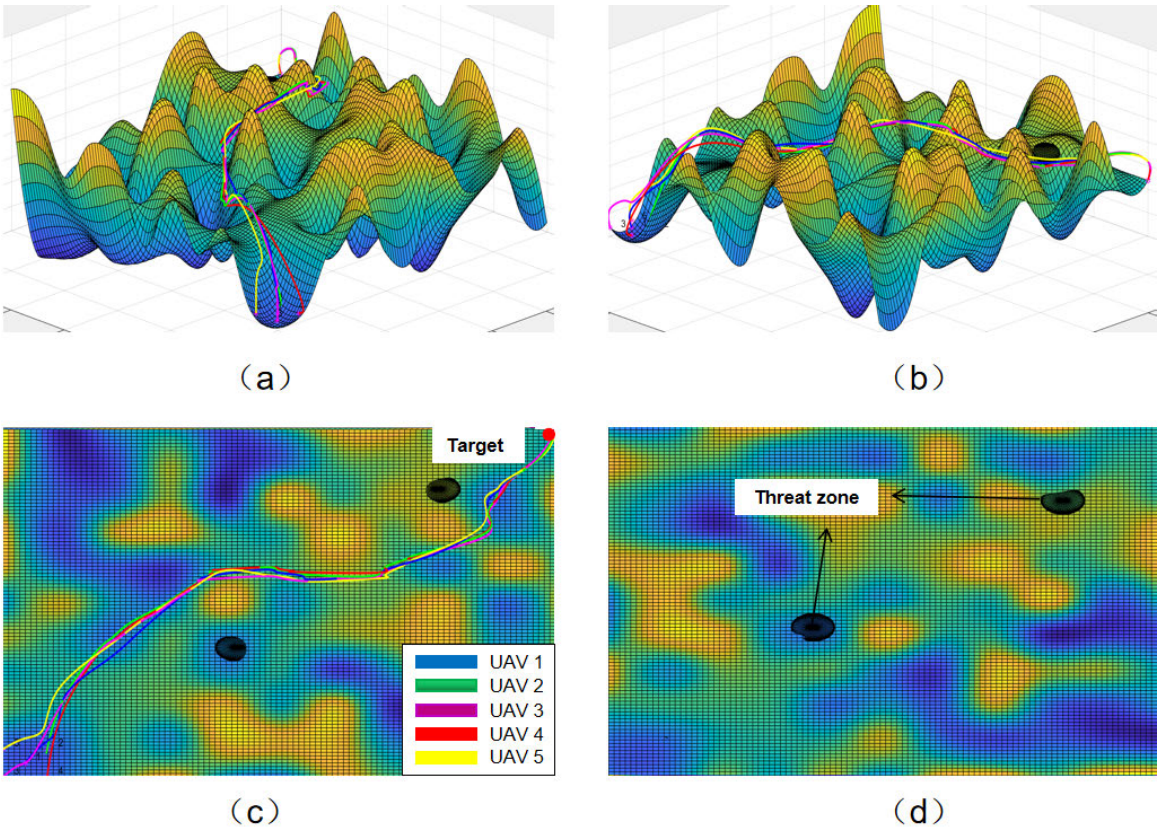

FIGURE 8. Path planning results of SSA. (a) view = (−45°, 45°), (b) =(45°, 45°), (c) =(90°, −90°), (d) =(0°, 90°).

the following points: (1) To compare the fairness of the experiment, the iterations of the three algorithms are all 40 times. At the beginning of the experiment, we tested each algorithm many times and set parameters such as population size as an optimal value obtained in the experiment. (2) To avoid the chance of experiment, each algorithm was tested 10 times in each environment. (3) In the discussion of the results, we took the length of the planned path and the success rate of the mission as the comparison items. The mission is considered successful when there is no collision.

Fig.9 shows the operation results of the fusion algorithm on six different environments. It can be seen from the figure that the fusion algorithm can pass through the mountainous environment constrained by various threatening regions without collision, including getting rid of the local minimum area and reaching the target position surrounded by obstacles. Table 3 is the mission success rate comparison of the three algorithms. Compared with ABC and DA algorithms, the fusion algorithm can adapt to various environments to complete tasks safely. Fig.10 is the comparison of the planned path length of the three algorithms. It can be concluded that the path length planned by the fusion algorithm is shorter and more stable. The above experiments can prove that compared with common path planning methods, the proposed fusion algorithm has better performance, stronger stability, and robustness.

TABLE 3. Path planning average success rate.

Test environment	ABC	DA	SSA
Env1	40%	70%	**100%**
Env2	10%	50%	**100%**
Env3	40%	60%	**100%**
Env4	60%	50%	**100%**
Env5	40%	60%	**100%**
Env6	50%	60%	**100%**

C. DYNAMIC ENVIRONMENT EXPERIMENT

To prove the dynamic obstacle avoidance capability of the proposed fusion algorithm, several dynamic flying obstacles are added in the static environment. In this simulation experiment, The mapping size of the 3-D mesh model is 60m * 60m * 60m, the distance of each adjacent neuron is 30m, and two dynamic obstacles are set, with starting coordinates of (30, 156, 380) and (101, 80, 350) and ending coordinates of (323, 313, 360) and (328, 227, 400). It can move at 5 m/s, which is slower than a UAV. There is one test UAV with a speed of 30 m/s. The starting coordinate is (20, 20, 200) and the target coordinate is (500, 500, 300). The results of the dynamic experiment are shown in Fig.12. In Fig.12 (a) and Fig.12 (b), it can be seen that the UAV detects obstacles at nodes (56, 117, 378) and (285, 288, 421), and then uses BINN to carry out local path replanning, finally arriving at the next node (100, 189, 326) and (337, 279, 426). In Fig.12 (c) and

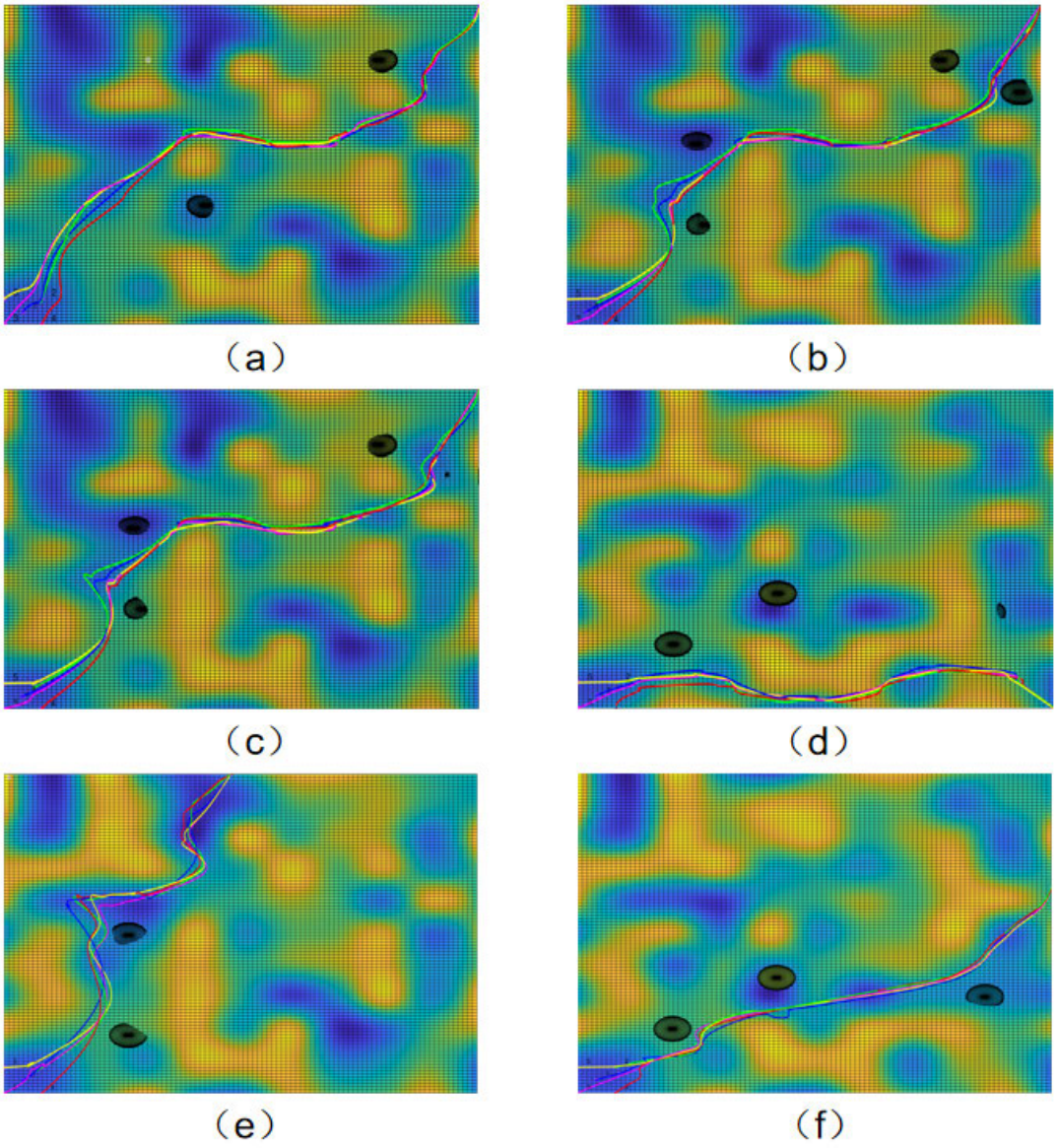

FIGURE 9. Path planning results of SSA in six environments. (a) Env1 (b) Env2 (c) Env3 (d) Env4 (e) Env5 (f) Env6.

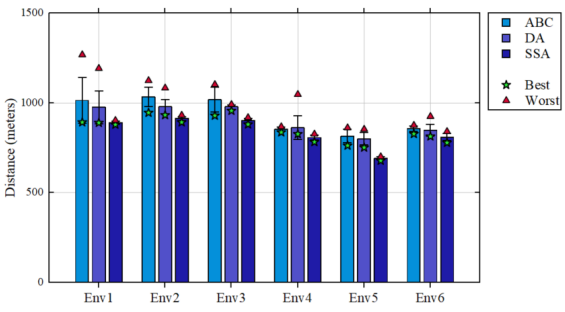

FIGURE 10. Path length results for the three different implementations: ABC, DA, SSA.

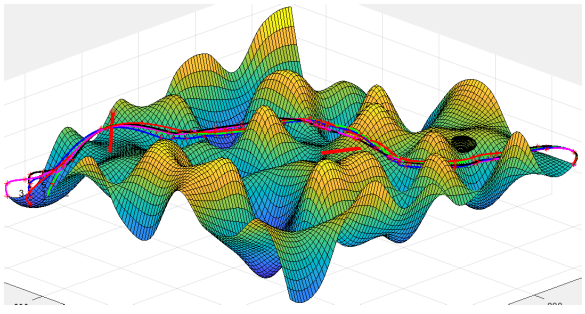

FIGURE 11. Dynamic obstacle avoidance of five UAVs.

Fig.12 (d), it can be seen that the UAV has completed obstacle avoidance without crashing into the mountain. The results show that the proposed method can avoid the obstacles when facing dynamic obstacles, and finally realize the collision-free flight.

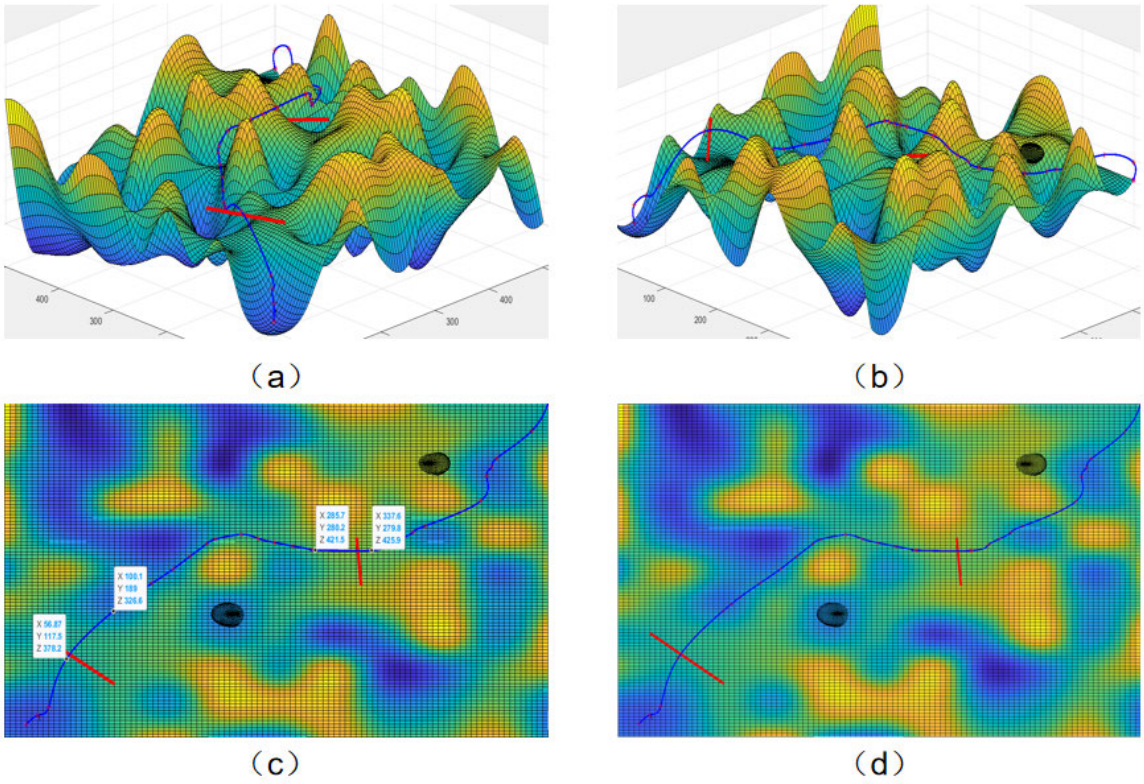

FIGURE 12. Dynamic obstacle avoidance simulation diagram of a single UAV. (a) view = (−45°, 45°), (b) =(45°, 45°), (c) =(0°, 90°), (d) =(0°, 90°) No marked.

TABLE 4. Simulation results of multi-UAV dynamic obstacle avoidance.

	Planned path length (m)	Flight duration(s)	Whether the crashing
UAV1	999.9579	33.3319	No
UAV2	954.5644	31.8188	No
UAV3	951.2191	31.7073	No
UAV4	955.2563	31.8418	No
UAV5	951.5356	31.7178	No

In order to prove that the proposed fusion algorithm can make multi-UAV avoid dynamic obstacles, four UAVs are added into the above experimental environment, and the starting coordinates of five UAVs are (20, 20, 200), (40, 40, 200), (0, 0, 200), (40, 0, 200), (0, 40, 200) respectively, the target coordinate is (500, 500, 300), the coordinate of the two threat zones are (210, 185), (390, 410), the threat radius is 20 meters. The experimental results are shown in Table 4 and Fig.11

The results show that the proposed method can avoid obstacles and achieve collision-free flight when multi-UAV faces dynamic obstacles. As shown in Fig.11, it can be seen that when the UAV detects an obstacle, it can avoid the dynamic obstacle and finally reach the target point.

D. DYNAMIC ENVIRONMENT CONTRAST EXPERIMENT

To demonstrate the effect of improving BINN, a comparative experiment was conducted. In this experiment, the proposed fusion algorithm is compared with the basic BINN, the starting coordinates of the five UAVs are (0, 250, 230), (0, 200, 230), (10, 225, 210), (20, 250, 210), (20, 200, 230) respectively. The target coordinate is (500, 250, 370), the coordinates of the two threat zones are (170, 260, 320), (460, 230, 380), and the threat radius is 20 meters. To improve the complexity of the environment, four dynamic obstacles were added, which are spheres with a radius of 5 meters, and their starting coordinates are (60, 200, 300), (150, 160, 400), (440, 270, 320), (400, 260, 390) respectively.

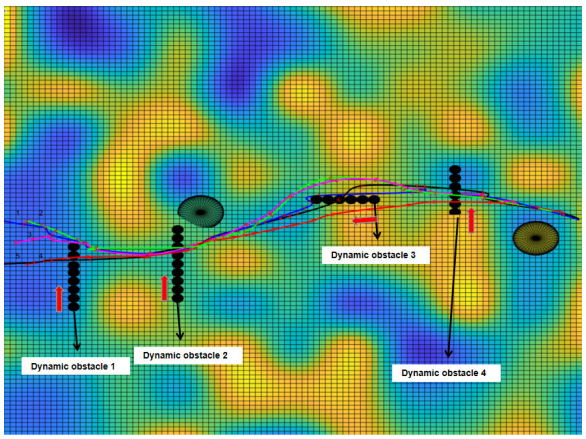

FIGURE 13. Path planning results of fusion algorithm in complex dynamic environment

The operation results of the proposed fusion algorithm are shown in Fig.13. It can be seen that the five UAVs can

TABLE 5. Comparison of path length and success rate in dynamic experiment.

	Planned path length(m)	success rate
Fusion algorithm	664.4867	100%
Basic BINN	830.6084	70%

safely avoid the dynamic obstacles flying either from the front or the side and have no collision with the mountain and the threat zones. Table 5 is the comparison of path length and obstacle avoidance success rate with the basic BINN, data from ten experiments on the same map. As can be seen from the table, the path length of the fusion algorithm is shorter, more stable, and the success rate reaches 100%. The above experiments show that compared with the basic BINN method, the proposed fusion algorithm is more stable in dynamic obstacle avoidance, and the planned path is shorter and better.

V. CONCLUSION

A fusion algorithm is proposed for path planning of multi-UAV in a mountainous environment. The fusion algorithm combines SSA, improved BINN, and B-spline curve to generate a safe, smooth, and short path for UAVs in the mountainous environment with radar threats, mountain threats, and dynamic obstacles. The main characteristic of the fusion algorithm is that it combines the advantages of the two methods, and the two methods promote each other. The sparrow search algorithm has the characteristics of fast convergence, high stability, and strong optimization performance, and the global route generated by the algorithm can guide for the improved BINN to avoid falling into the local optimal. Then, the structure of the traditional BINN is improved by adding a layer of buffer to improve the success rate of avoiding dynamic obstacles.

Experimental results in different static and dynamic environments show that the proposed fusion algorithm can effectively solve the path planning problem of multi-UAV in a complex mountainous environment. In the static environment experiment, we compared several common path planning methods, such as ABC and DA, and showed obvious advantages in terms of safety and path length. In dynamic environment experiments, compared with basic BINN, the improved BINN has obvious progress in path planning length and obstacle avoidance success rate. Therefore, the fusion algorithm proposed in this paper is very suitable for multi-UAV path planning in a complex mountainous environment.

In the future, UAVs will be used more for reconnaissance or navigation missions in complex environments. In the case of known target coordinates, the global path planning method is undoubtedly the best choice, and its planned path is better and shorter than the local path planning. Because of the complexity of the environment, there is a great chance that the UAV will carry out the replanning of the flight path under the predetermined trajectory, and local planning is an indispensable part. The combination of global path planning and local path planning can reduce the computing power requirement of airborne computers and is more suitable for practical applications. Therefore, the combination of global planning methods and local planning methods is a better solution for multi-UAV path planning in a long-distance and complex environment.

REFERENCES

[1] P. Xiao, L. Wang, J. Chuan, X. Wang, J. Kuang, and A. Fei, "Implementation for UAVs aided edge sensing system in wireless emergency communications," in *Proc. 11th Int. Conf. Wireless Commun. Signal Process. (WCSP)*, Oct. 2019, pp. 1–5.
[2] J. Wang, K. Liu, and J. Pan, "Online UAV-mounted edge server dispatching for mobile-to-mobile edge computing," *IEEE Internet Things J.*, vol. 7, no. 2, pp. 1375–1386, Feb. 2020.
[3] S. Aggarwal and N. Kumar, "Path planning techniques for unmanned aerial vehicles: A review, solutions, and challenges," *Comput. Commun.*, vol. 149, pp. 270–299, Jan. 2020.
[4] S. Yin, S. Zhao, Y. Zhao, and F. R. Yu, "Intelligent trajectory design in UAV-aided communications with reinforcement learning," *IEEE Trans. Veh. Technol.*, vol. 68, no. 8, pp. 8227–8231, Aug. 2019.
[5] S. Gao, J. Wu, and J. Ai, "Multi-UAV reconnaissance task allocation for heterogeneous targets using grouping ant colony optimization algorithm," *Soft Comput.*, vol. 25, no. 10, pp. 7155–7167, May 2021.
[6] M. A. Khan, I. M. Qureshi, and F. Khanzada, "A hybrid communication scheme for efficient and low-cost deployment of future flying ad-hoc network (FANET)," *Drones*, vol. 3, no. 1, p. 16, 2019.
[7] J. Li, Y. Xiong, J. She, and M. Wu, "A path planning method for sweep coverage with multiple UAVs," *IEEE Internet Things J.*, vol. 7, no. 9, pp. 8967–8978, Sep. 2020.
[8] Y. Wang, Y. Yue, M. Shan, L. He, and D. Wang, "Formation reconstruction and trajectory replanning for multi-UAV patrol," *IEEE/ASME Trans. Mechatronics*, vol. 26, no. 2, pp. 719–729, Apr. 2021.
[9] L. Xiaolei, J. Lin, J. Zufei, and G. Chen, "Mobile robot path planning based on environment modeling of grid method in unstructured environment," *Mach. Tool Hydraul.*, vol. 4, no. 16, pp. 1–6, 2016.
[10] D. Shiyou, Z. Xiaoping, and L. Guoqing, "Cooperative planning method for swarm UAVs based on hierarchical strategy," in *Proc. 3rd Int. Conf. Syst. Sci., Eng. Design Manuf. Inf.*, vol. 2, Oct. 2012, pp. 304–307.
[11] D. Wang, S. Chen, Y. Zhang, and L. Liu, "Path planning of mobile robot in dynamic environment: Fuzzy artificial potential field and extensible neural network," *Artif. Life Robot.*, vol. 26, no. 1, pp. 129–139, Feb. 2021.
[12] J. Xie, L. R. G. Carrillo, and L. Jin, "An integrated traveling salesman and coverage path planning problem for unmanned aircraft systems," *IEEE Control Syst. Lett.*, vol. 3, no. 1, pp. 67–72, Jan. 2019.
[13] Z. Biao, C. Qixin, and W. Wenshan, "An algorithm for mobile robot path planning based on 3D grid map," *J. Xi'an Jiaotong Univ.*, vol. 47, no. 10, pp. 57–61, 2013.
[14] Z. Lv, L. Yang, Y. He, Z. Liu, and Z. Han, "3D environment modeling with height dimension reduction and path planning for UAV," in *Proc. 9th Int. Conf. Model., Identificat. Control (ICMIC)*, Jul. 2017, pp. 734–739.
[15] N. Junlan, Z. Qingjie, and W. Yanfen, "UAV path planning based on weighted-Voronoi diagram," *Flight Dyn.*, vol. 33, pp. 339–343, Jan. 2015.
[16] T. Zhang, Y. Zhu, and J. Song, "Real-time motion planning for mobile robots by means of artificial potential field method in unknown environment," *Ind. Robot, Int. J.*, vol. 37, no. 4, pp. 384–400, 2010.
[17] N. K. A. Shubhani, "Path planning for mobile robot based on improved artificial potential field method in complex environment," *Comput. Commun.*, vol. 24, pp. 45–48, Oct. 2013.
[18] Y. Du, X. Zhang, and Z. Nie, "A real-time collision avoidance strategy in dynamic airspace based on dynamic artificial potential field algorithm," *IEEE Access*, vol. 7, pp. 169469–169479, 2019.
[19] H. Xudong and R. Yuhan, "Trajectory planning technology for low-altitude penetration of drones," *J. Comput. Eng. Appl.*, vol. 37, no. 12, pp. 25–30 and 66, 2020.
[20] H. Zhizhong, X. Kehu, and S. Chunlin, "Smoothing of digital terrain for low-altitude penetration," *J. Nanjing Univ. Aeronaut. Astronaut.*, no. 5, pp. 493–498, 2000.
[21] Y. D. Sergeyev, D. Kvasov, and M. Mukhametzhanov, "On the efficiency of nature-inspired metaheuristics in expensive global optimization with limited budget," *Sci. Rep.*, vol. 8, no. 1, 2018, Art. no. 453.

[22] K. Sharma, S. Singh, and R. Doriya, "Optimized cuckoo search algorithm using tournament selection function for robot path planning," *Int. J. Adv. Robot. Syst.*, vol. 18, no. 3, May 2021, Art. no. 172988142199613.
[23] X. Zhou, F. Gao, X. Fang, and Z. Lan, "Improved bat algorithm for UAV path planning in three-dimensional space," *IEEE Access*, vol. 9, pp. 20100–20116, 2021.
[24] W. Zhang, S. Zhang, F. Wu, and Y. Wang, "Path planning of UAV based on improved adaptive grey wolf optimization algorithm," *IEEE Access*, vol. 9, pp. 89400–89411, 2021.
[25] Y. Cao, W. Wei, and Y. Bai, "Multi-base multi-UAV cooperative reconnaissance path planning with genetic algorithm," *Cluster Comput.*, vol. 22, pp. 5175–5184, May 2019.
[26] L. Wang, L. Liu, J. Qi, and W. Peng, "Improved quantum particle swarm optimization algorithm for offline path planning in AUVs," *IEEE Access*, vol. 8, pp. 143397–143411, 2020.
[27] C. J. QI Xuanxuan and H. Jiajun, "Path planning for unmanned vehicle based on improved A* algorithm," *J. Comput. Appl.*, vol. 40, no. 7, pp. 2021–2027, 2020.
[28] P. Wang, X. Bai, and C.-C. Xie, "3D multi-UAV collaboration based on the hybrid algorithm of artificial bee colony and A," *Aerosp. Control*, vol. 37, no. 6, pp. 29–34 and 65, Dec. 2019.
[29] Z. Li, Z. Zhang, H. Liu, and L. Yang, "A new path planning method based on concave polygon convex decomposition and artificial bee colony algorithm," *Int. J. Adv. Robotic Syst.*, vol. 17, no. 1, 2020, Art. no. 1729881419894787.
[30] U. Orozco-Rosas, K. Picos, and O. Montiel, "Hybrid path planning algorithm based on membrane pseudo-bacterial potential field for autonomous mobile robots," *IEEE Access*, vol. 7, pp. 156787–156803, 2019.
[31] L. Chang, L. Shan, C. Jiang, and Y. Dai, "Reinforcement based mobile robot path planning with improved dynamic window approach in unknown environment," *Auto. Robots*, vol. 45, no. 1, pp. 51–76, Jan. 2021.
[32] J. Xue and B. Shen, "A novel swarm intelligence optimization approach: Sparrow search algorithm," *Syst. Sci. Control Eng.*, vol. 8, no. 1, pp. 22–34, Jan. 2020.
[33] S. X. Yang and M. Q. H. Meng, "Real-time collision-free motion planning of a mobile robot using a neural dynamics-based approach," *IEEE Trans. Neural Netw.*, vol. 14, no. 6, pp. 1541–1552, Nov. 2003.
[34] C. Balta, S. Ozturk, M. Kuncan, and I. Kandilli, "Dynamic centripetal parameterization method for B-spline curve interpolation," *IEEE Access*, vol. 8, pp. 589–598, 2020.
[35] C. Q. W. X. LI Yali and W. Shuqin, "Comparative study of several new swarm intelligence optimization algorithms," *J. Comput. Eng. Appl.*, vol. v.56;No.965, no. 22, pp. 7–18, 2020.
[36] A. L. Hodgkin and A. F. Huxley, "A quantitative description of membrane current and its application to conduction and excitation in nerve," *J. Physiol.*, vol. 117, pp. 500–544, Aug. 1952.
[37] S. Grossberg, "Nonlinear neural networks: Principles, mechanisms, and architectures," *Neural Netw.*, vol. 1, no. 1, pp. 17–61, 1988, doi: 10.1016/0893-6080(88)90021-4.
[38] A. R. Willms and S. X. Yang, "An efficient dynamic system for real-time robot-path planning," *IEEE Trans. Syst., Man, Cybern. B. Cybern.*, vol. 36, no. 4, pp. 755–766, Aug. 2006.
[39] J. Ni, X. Wang, M. Tang, W. Cao, P. Shi, and S. X. Yang, "An improved real-time path planning method based on dragonfly algorithm for heterogeneous multi-robot system," *IEEE Access*, vol. 8, pp. 140558–140568, 2020.

QINGLI LIU received the Ph.D. degree from Northeast University, China, in 2012. Since 2019, he has been a Professor with the Information Engineering College, Dalian University. He was a Visiting Scholar with the Department of Electronic Engineering, Utah State University, from September 2015 to March 2016. His current research interests include satellite networks, wireless communication, and unmanned aerial vehicle systems.

YANG ZHANG received the B.S. degree in optoelectronics information science and engineering from Wuchang Shouyi University, Wuhang, China, in 2019. He is currently pursuing the master's degree with the Communication and Network Laboratory, Dalian University. His current research interests include UAV networking technology and UAV path planning.

MENGQIAN LI received the B.S. degree in computer science and technology from Taiyuan University, Anshan, China, in 2019. She is currently pursuing the master's degree with the Communication and Network Laboratory, Dalian University. Her current research interests include UAV networking technology and UAV task assignment.

ZHENYA ZHANG received the B.S. degree in the Internet of Things from Henan University of Science and Technology, Luoyang, China, in 2019. She is currently pursuing the master's degree with the Communication and Network Laboratory, Dalian University. Her current research interests include UAV networking technology and UAV task assignment.

NA CAO received the B.S. degree in computer science and technology from Zaozhuang University, Anshan, China, in 2020. She is currently pursuing the master's degree with the Communication and Network Laboratory, Dalian University. Her current research interests include UAV networking technology and UAV task assignment.

JIALE SHANG received the B.S. degree in computer science and technology from Dalian University, Dalian, China, in 2019. She is currently pursuing the master's degree with the Communication and Network Laboratory, Dalian University. Her current research interests include UAV networking technology and UAV task assignment.